

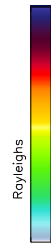
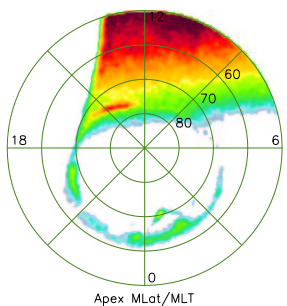
The Conjugacy of Dayside Auroral Electron Precipitation (Particularly the 15 MLT Bright Spot)

M. O. Fillingim, G. K. Parks, Y.-K. Tung, M. Wilber,
T. Immel, S. B. Mende

Space Sciences Laboratory, University of California, Berkeley

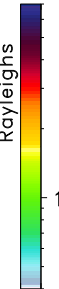
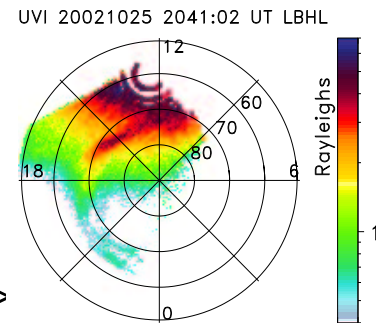
Yosemite Conference–Workshop 2003
Dayside Magnetopause and Cusp
Yosemite National Park, CA
February 9 – 13, 2003

FUV Imagers/WIC 25 Oct 2002
20:41:18 UT



Northern Hemisphere
<--- (IMAGE)

Southern Hemisphere
(POLAR) --->



Introduction

The 15 MLT bright spot

- . is centered near 15 MLT and 75° ILAT
- . is persistent
 - . auroral image data [*Cogger et al.*, 1977; *Anger et al.*, 1989; *Liou et al.*, 1997]
 - . particle measurements [*McDiarmid et al.*, 1975; *Evans*, 1985; *Newell et al.*, 1996]
- . has a LLBL [*Lundin and Evans*, 1985] or plasma sheet source [*Liou et al.*, 1999]
- . statistically maps to the Region 1 upward current region [*Iijima and Potemra*, 1976]
- . is influenced by IMF and solar wind [*Murphree et al.*, 1981; *Vo and Murphree*, 1995]
- . is dynamic [*Anger et al.*, 1987, *Lui et al.*, 1987]
⇒ K–H instability [*Lui et al.*, 1989]

Introduction (cont'd)

The 15 MLT bright spot

- displays seasonal variability [*Liou et al.*, 2001]
- conductivity/M–I coupling may play a role
- seasonal/hemispheric differences
⇒ conjugacy

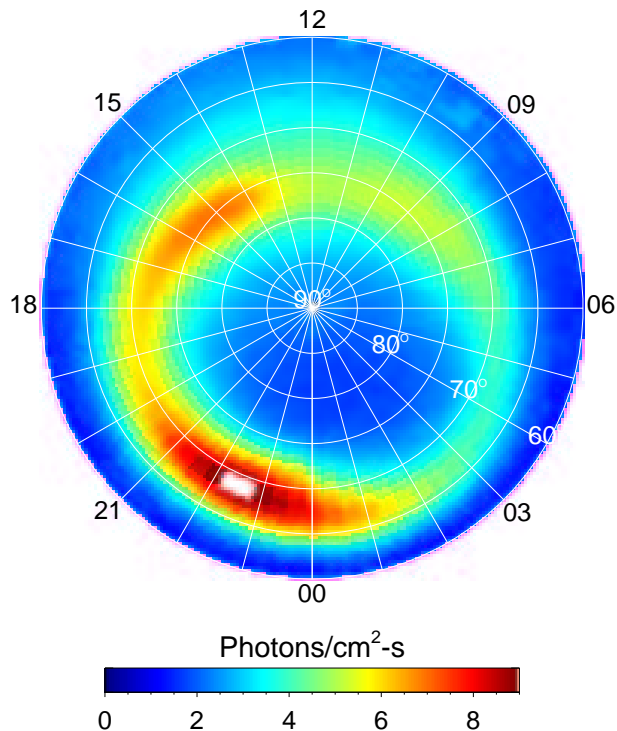


Figure 1. A map of average northern auroral intensity at LBH-long band ($\lambda \sim 1700 \text{ \AA} \pm 50 \text{ \AA}$) in the geomagnetic latitude-local time format. Contours of magnetic latitudes are drawn from 60° (outermost edge of the plot) to 90° (center of the plot) with an increment of 5° . Local times are hourly drawn and marked counter-clockwise along the 60° magnetic latitude for every 3 hours starting at 0000 MLT on the bottom of the plot.

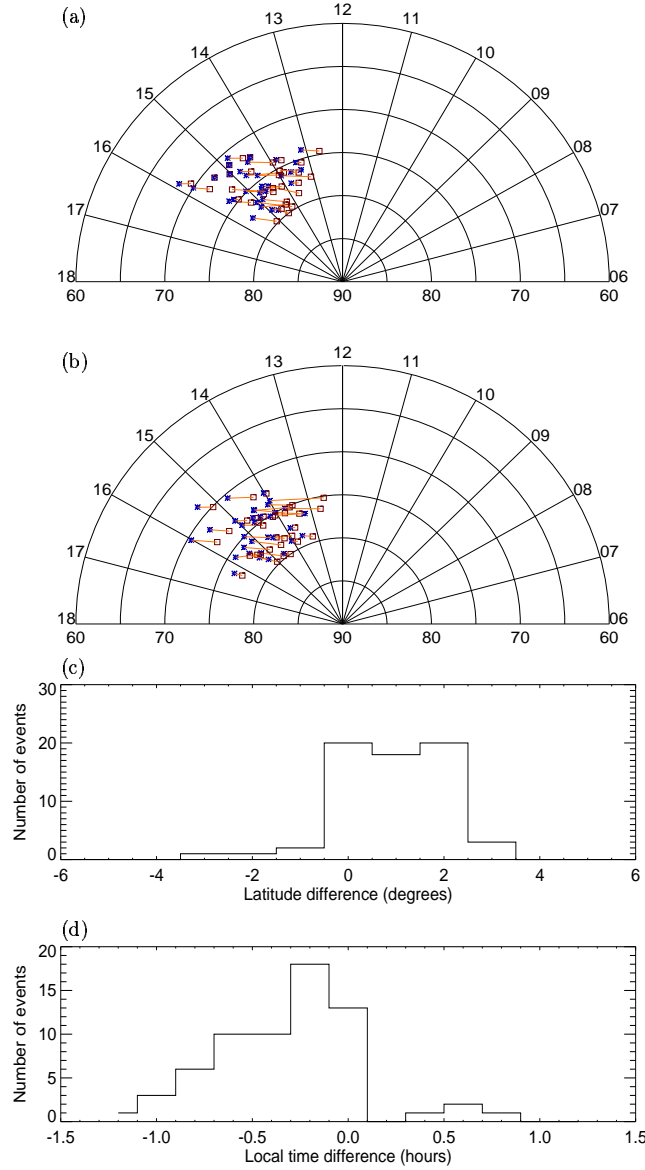
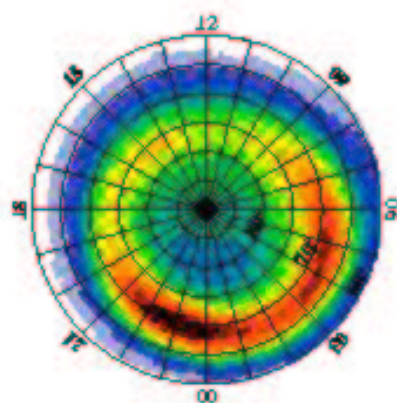
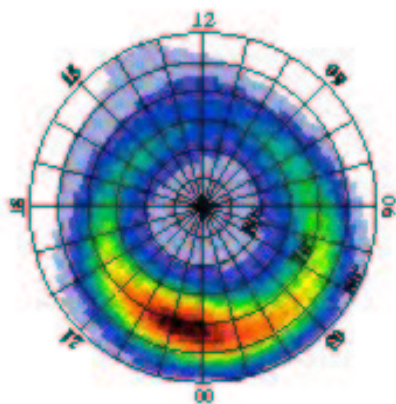


Plate 7. A distribution of the 65 simultaneous measurement events from the (a) Polar UVI and (b) DMSP F13. The blue crosses correspond to the locations where peak in electron energy flux was identified and the red boxes correspond to the locations of where interfaces between the plasma sheet and other regions are located by the DMSP F13 satellite. The two symbols are connected by an orange line indicating the satellite trajectory. (c) The histogram of the bright spot events with respect to the latitude (local time) difference between the two locations plotted in Plate 7a. A positive (negative) value in the latitude (local time) difference indicates that peak electron energy flux was found equatorward (westward) of the plasma sheet boundary.

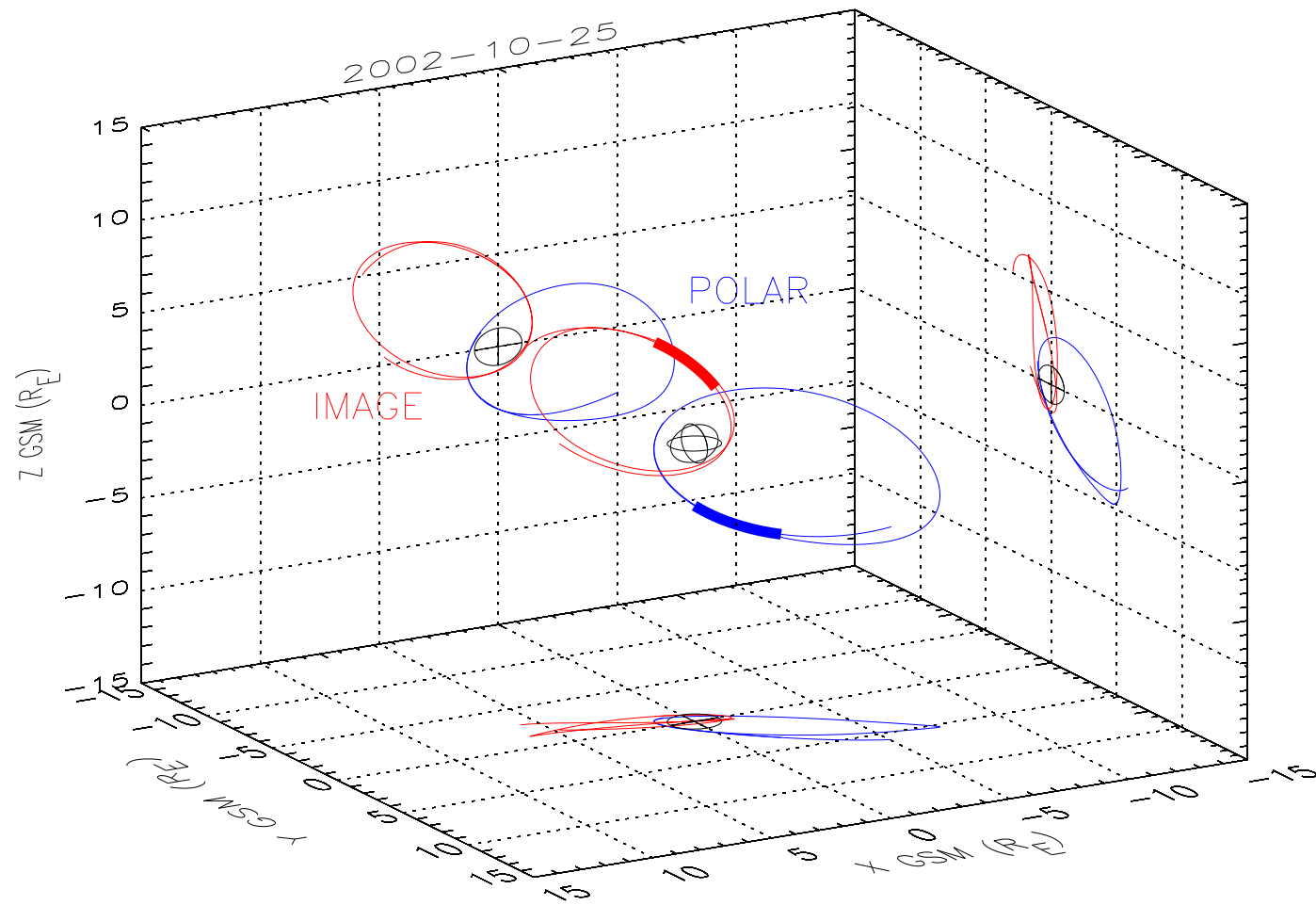
Summer



Winter

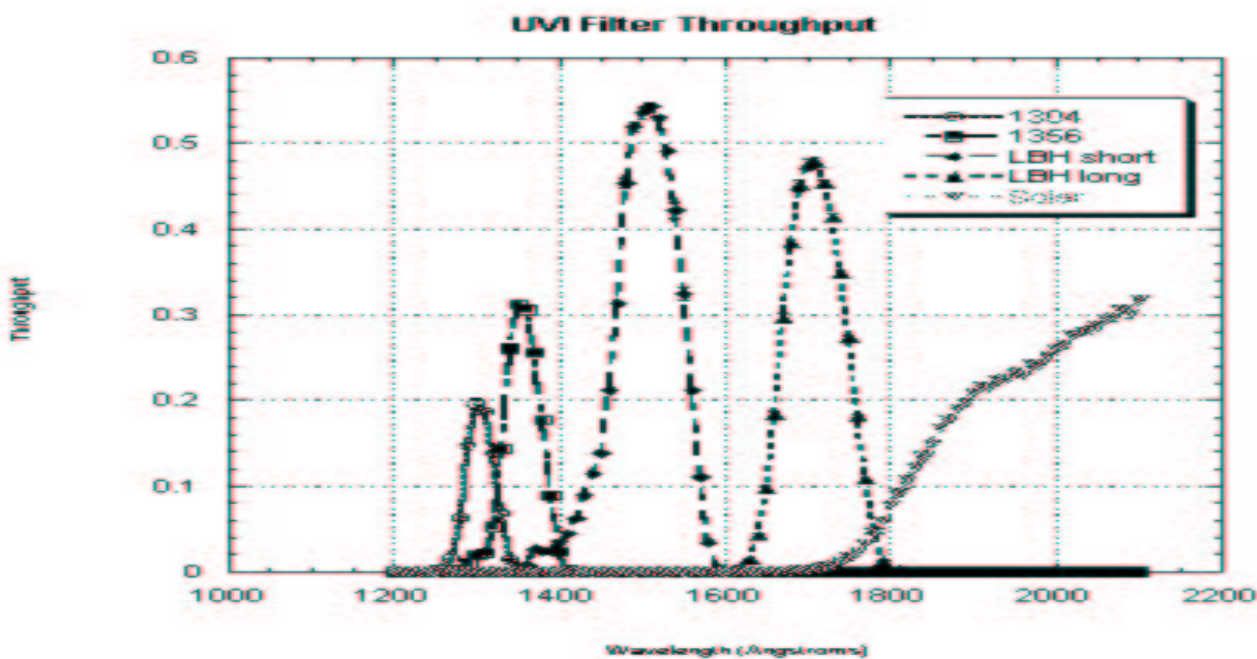


Spacecraft Orbits



Instrumentation

- Integration time
 - UVI: ~ 37 seconds (or 18 seconds) continuous (multiple modes of operation)
 - WIC: ~ 10 seconds every ~ 2 minutes
- Field-of-view
 - UVI: ~ 8°
 - WIC: ~ 17°
- Pixel resolution at apogee
 - UVI: ~ 30 km
 - WIC: ~ 50 km



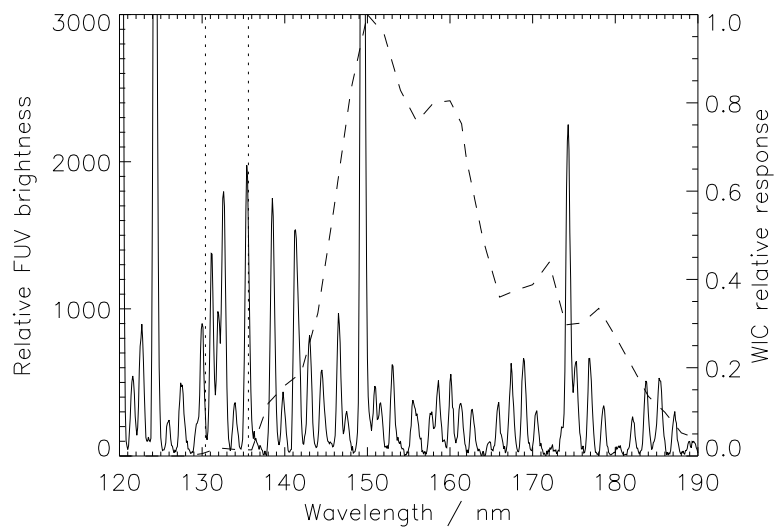
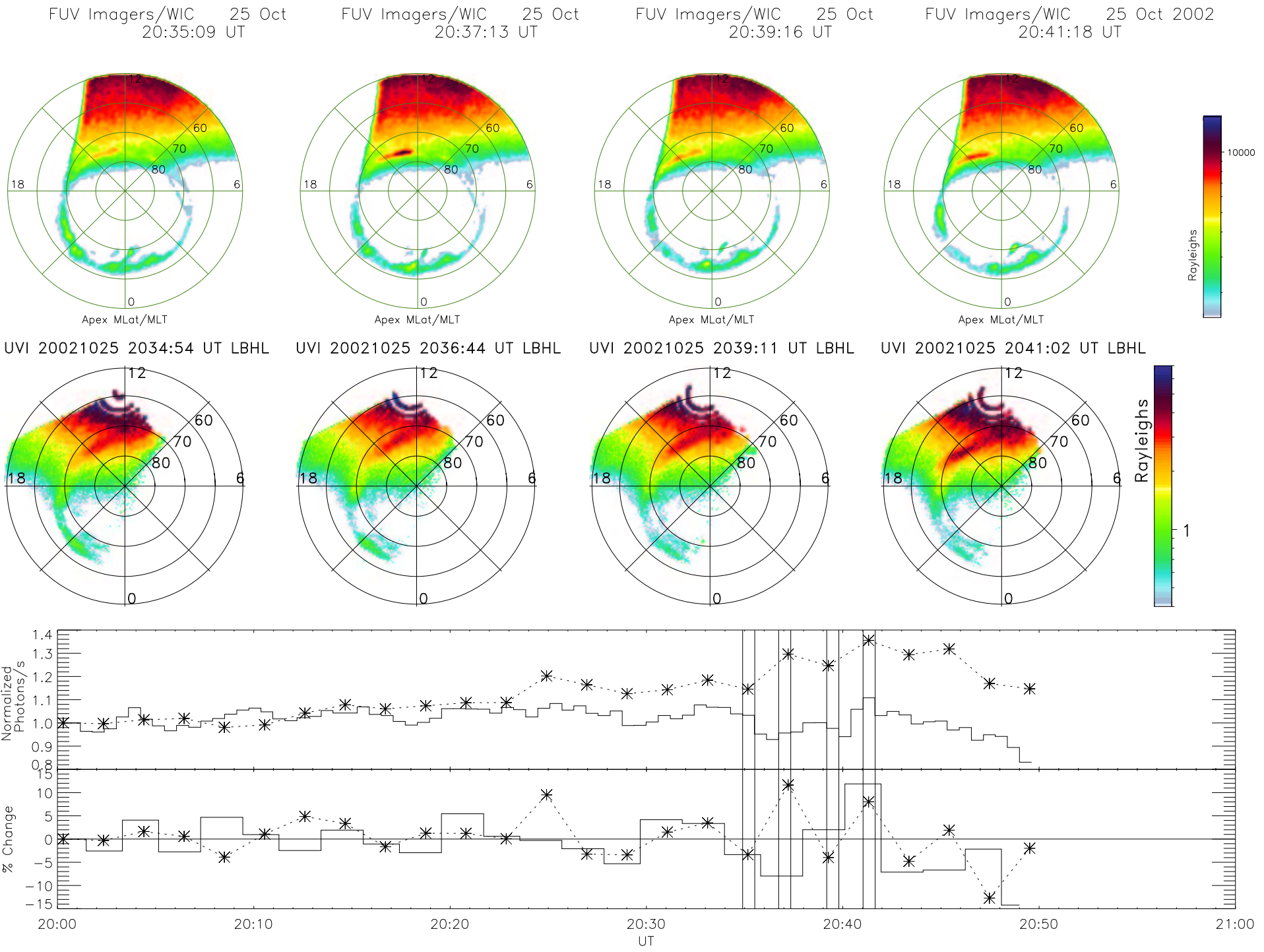
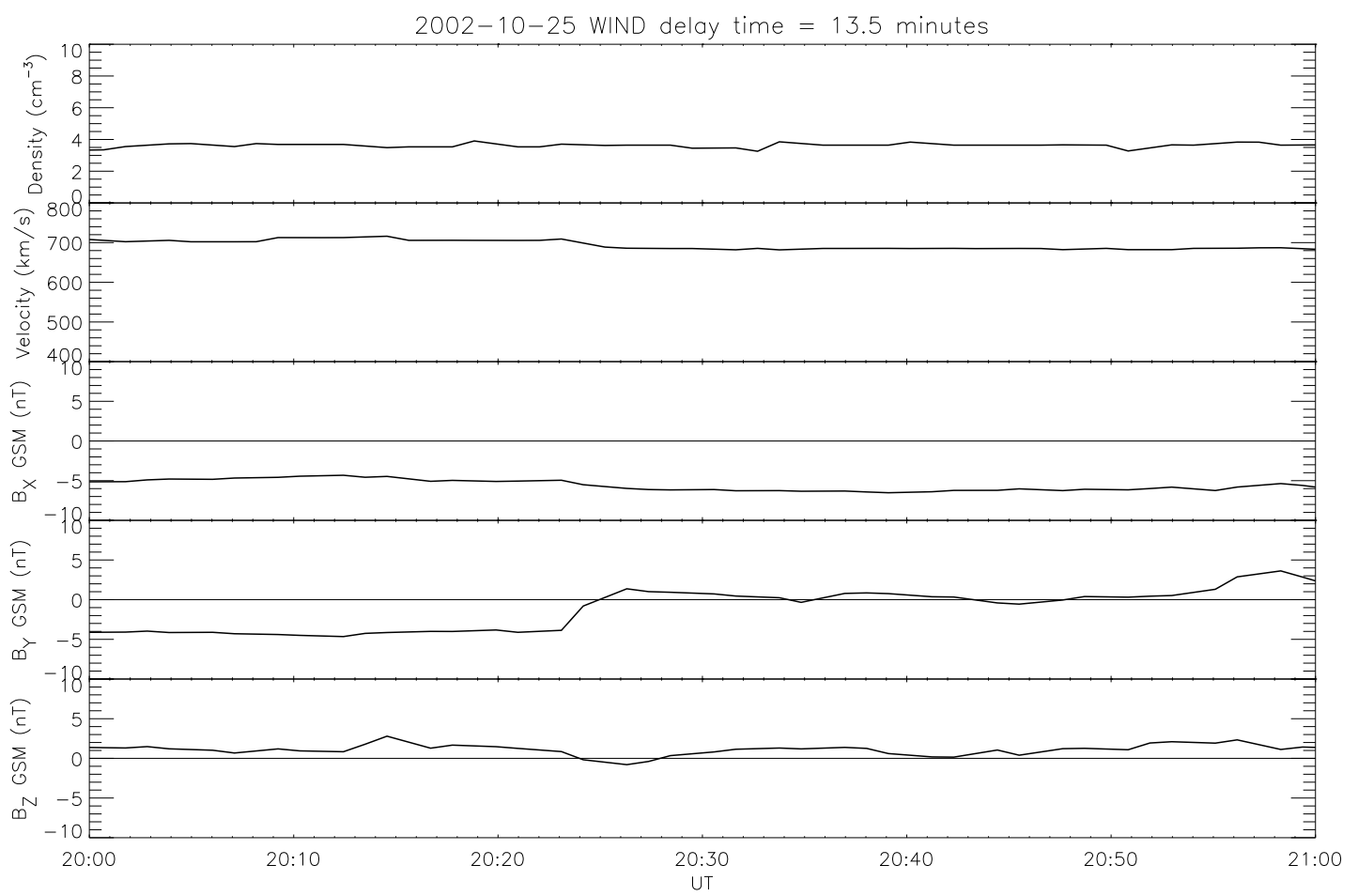
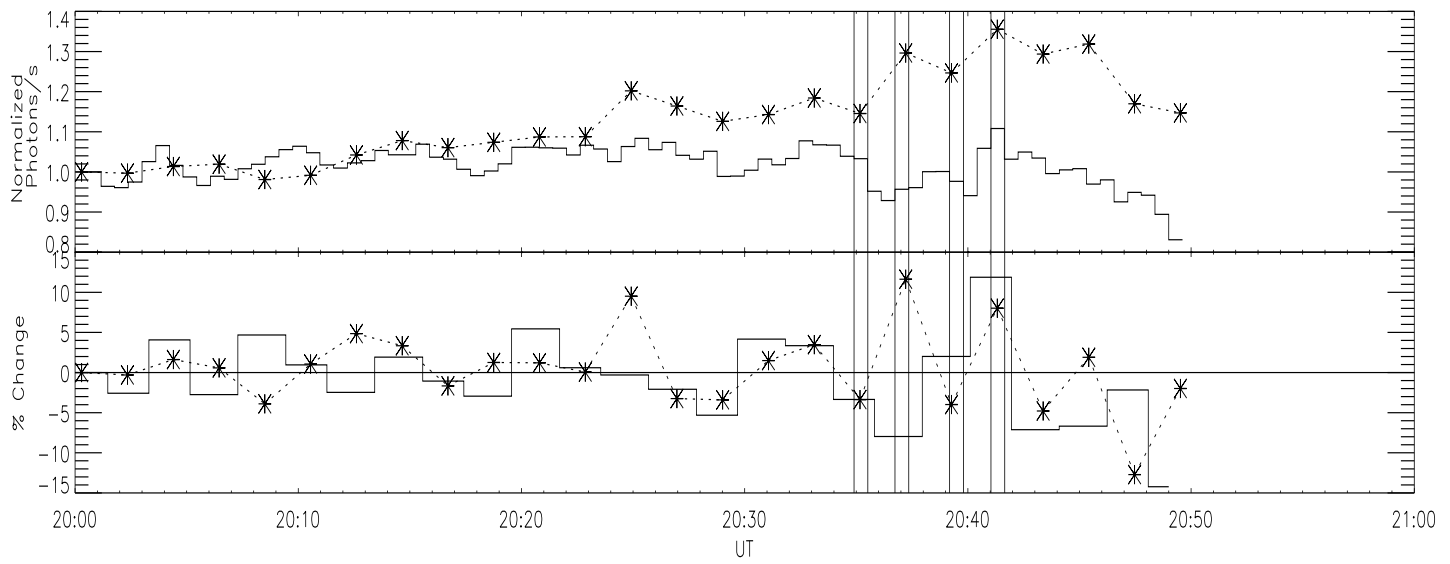


Figure 3. Laboratory spectrum of FUV emission from N_2 (Ajello and Shemansky, 1985) and WIC relative spectral response (dashed line). Dotted lines indicate the location of oxygen emissions at 130.4 nm and 135.6 nm.

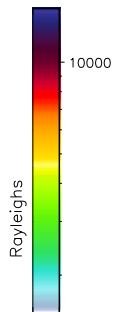
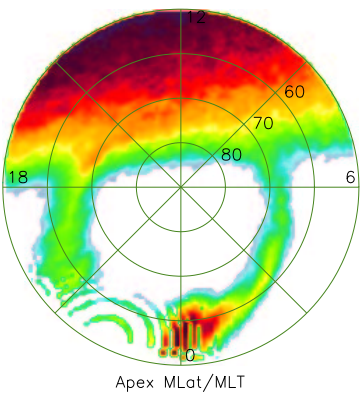
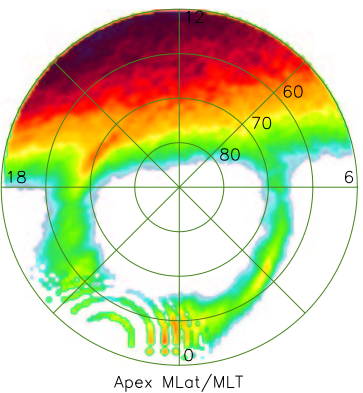
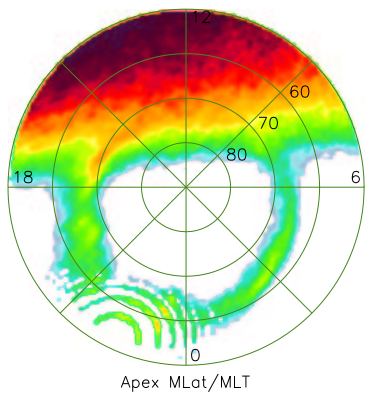




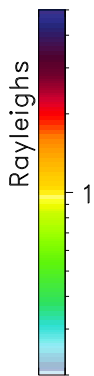
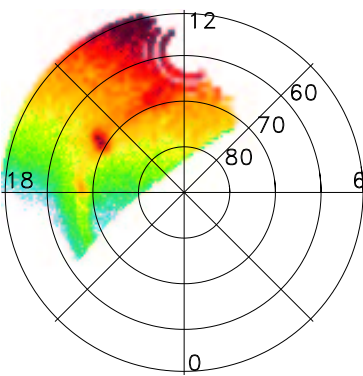
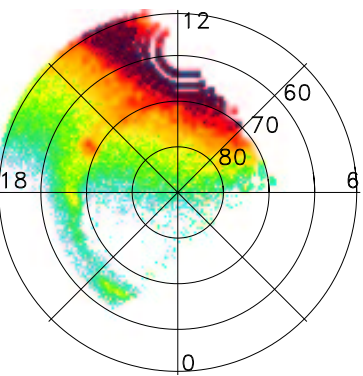
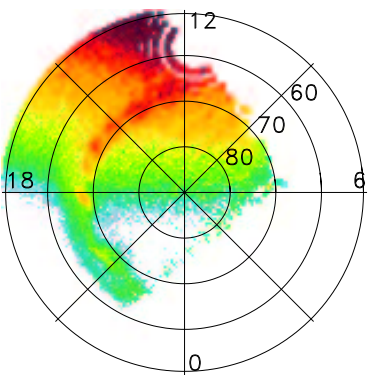
FUV Imagers/WIC 04 Nov
19:09:52 UT

FUV Imagers/WIC 04 Nov
19:13:58 UT

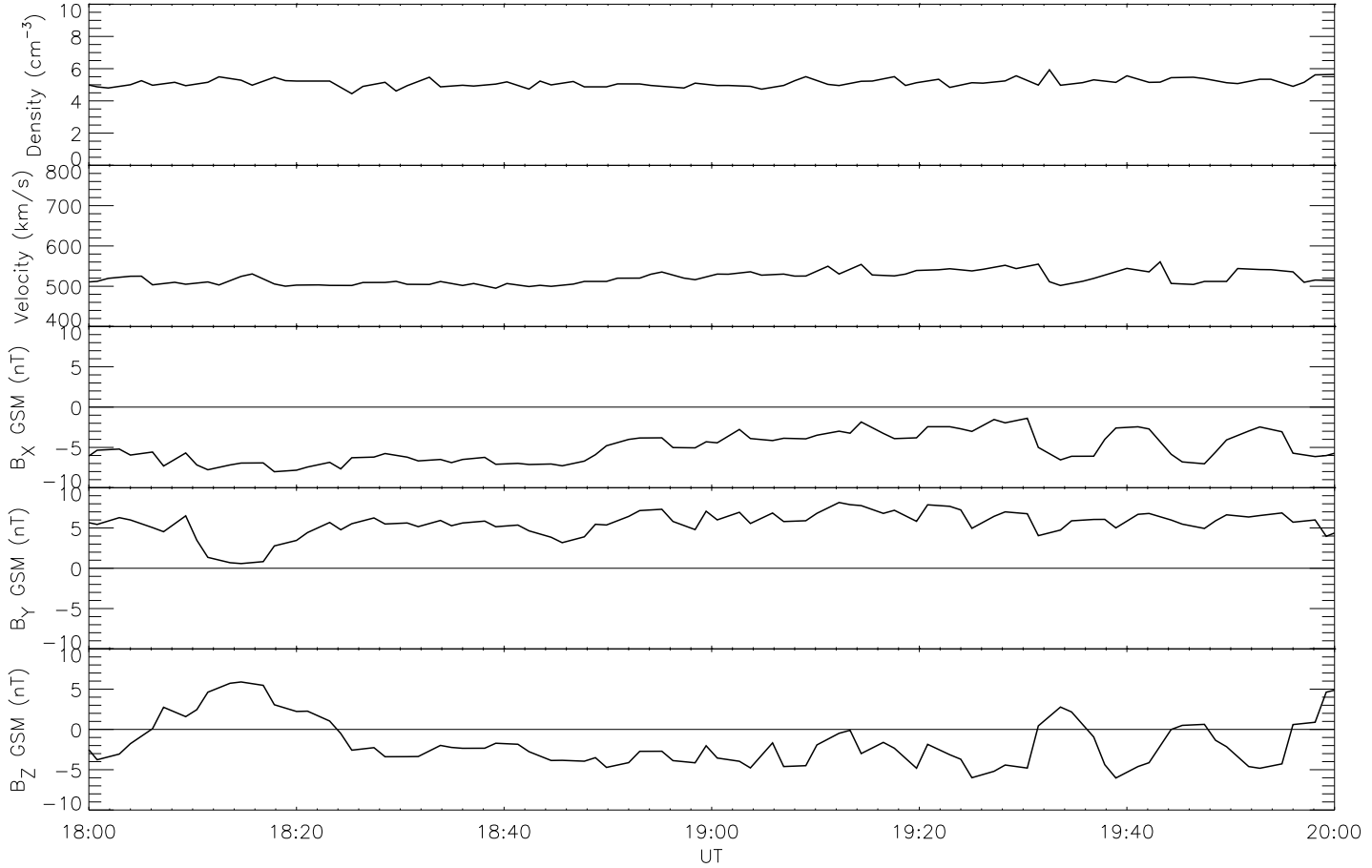
FUV Imagers/WIC 04 Nov 2002
19:16:01 UT



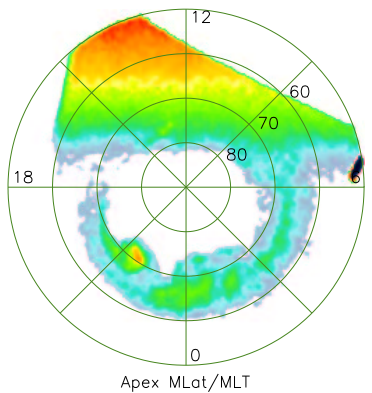
UVI 20021104 1909:29 UT LBHS UVI 20021104 1914:04 UT LBHL UVI 20021104 1915:37 UT LBHS



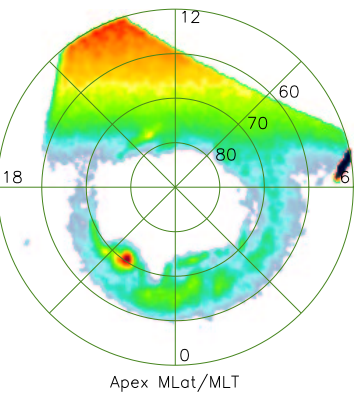
2002-11-04 WIND delay time = 12 minutes



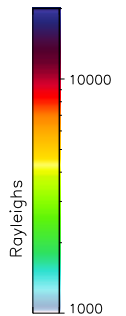
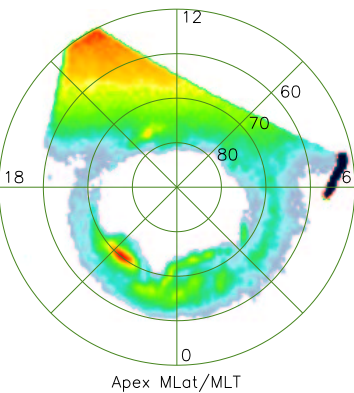
FUV Imagers/WIC 05 Nov
13:03:45 UT



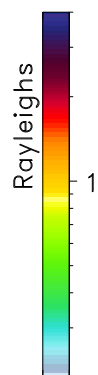
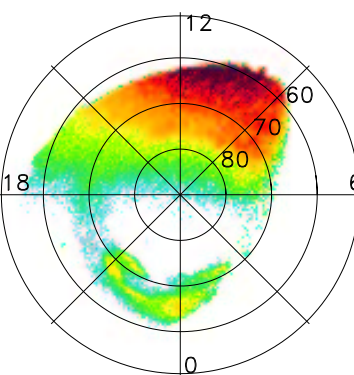
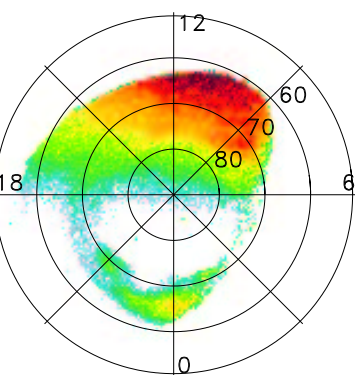
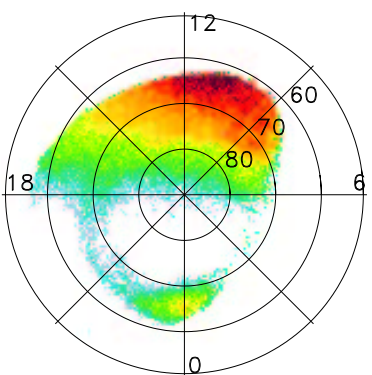
FUV Imagers/WIC 05 Nov
13:05:48 UT



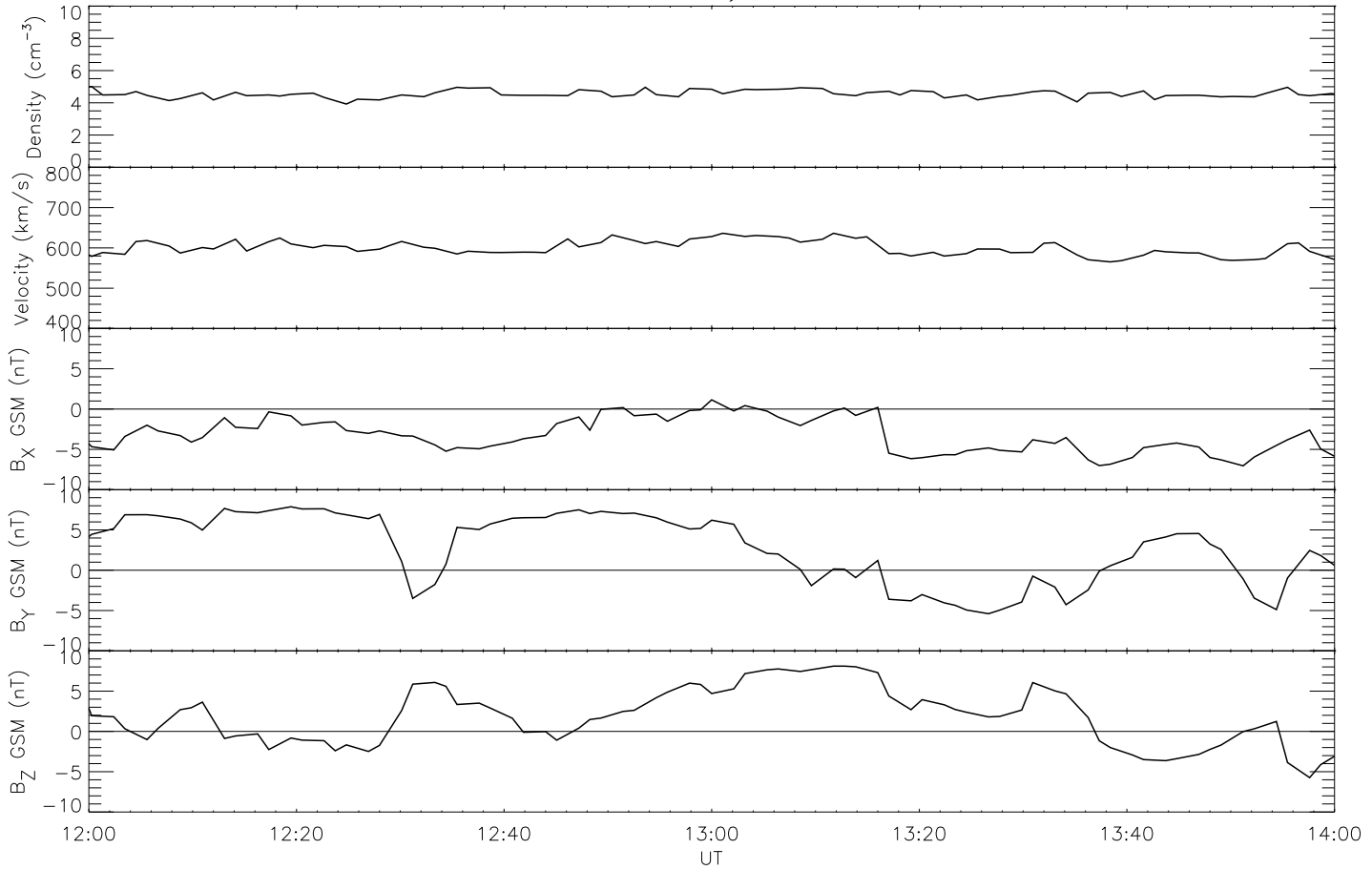
FUV Imagers/WIC 05 Nov 2002
13:07:52 UT



UVI 20021105 1303:26 UT LBHL UVI 20021105 1305:53 UT LBHL UVI 20021105 1307:43 UT LBHL



2002-11-05 WIND delay time = 12 minutes



Summary

- . Temporal differences between northern and southern hemispheres
- . Morphological/spatial differences between hemispheres

⇒ Non-conjugacy in particle source, current source,
&/or acceleration mechanism

$$J_{\parallel} \Leftrightarrow \text{change in vorticity, } \Omega$$

- . Can K–H instability explain these observations?
- . Differences in ionospheric conductivity --- What effect?

Future Work

- . Statistical studies/correlations with IMF and solar wind conditions
- . Seasonal variations
- . Investigations into source mechanism
- . Dayglow removal
- . Substorm activity
-
- . Identical instrumentation observing both hemispheres simultaneously
 - . time resolution
 - . spectral resolution
 - . spatial resolution